Compact and Lightweight Additive Manufactured Parallel-Plate Waveguide Half-Luneburg Geodesic Lens Multiple-Beam Antenna in the K_a-Band

José Rico-Fernández, Freysteinn V. Vidarsson, *Graduate Student Member, IEEE*, Manuel Arrebola, *Senior Member, IEEE*, Nelson J. G. Fonseca, *Senior Member, IEEE*, and Oscar Quevedo-Teruel, *Fellow, IEEE*

***Abstract*—In this letter, a parallel-plate waveguide half-Luneburg geodesic lens multiple-beam antenna optimized for additive manufacturing is designed and validated experimentally in the K_a-band. Two prototypes were manufactured in $AlSi_{10}Mg$ through laser powder-bed fusion and measured in an anechoic chamber. The compact and lightweight prototype optimized for additive manufacturing demonstrates excellent RF performance while significantly reducing mass and mechanical complexity. Specifically, misalignment errors present in previous studies are solved, improving sidelobe level by up to 10 dB. A maximum realized gain of 22.1 dBi is measured at 28 GHz. This single-piece, compact, and lightweight design is particularly attractive for applications having mass restrictions and limited space like millimeter-wave systems on board small satellites.**

***Index Terms*—Additive manufacturing, geodesic lens, half-Luneburg lens, lens antenna, millimeter-wave, multiple beam antenna, parallel-plate waveguide.**

I. Introduction

IN RECENT years, there has been a growth in the development of radiofrequency (RF) components in the millimeter-wave (mmWave) band. Quasi-optical systems have attracted interest due to their high directivity and simple feeding network [1]. In particular, some solutions have been developed based on planar beamformers, such as Luneburg lenses [2], [3], Rotman lenses [4], [5], [6], [7], and pillbox antennas [8], [9], [10]. These technologies were aimed at future generations of cellular networks and satellite communication systems [11], [12].

Manuscript received 2 September 2022; revised 17 October 2022; accepted 10 November 2022. Date of publication 15 November 2022; date of current version 7 April 2023. The work of Manuel Arrebola was supported in part by Grant MCIN/AEI/10.13039/501100011033 within the project PID2020-114172RB-C21. *(Corresponding author: Oscar Quevedo-Teruel.)*

José Rico-Fernández is with The Next Pangea, THENEXTPANGEA SL, 33418 Asturias, Spain (e-mail: pepe.rico@thenextpangea.com).

Freysteinn V. Vidarsson and Oscar Quevedo-Teruel are with the Division of Electromagnetic Engineering, KTH Royal Institute of Technology, SE-100 44 Stockholm, Sweden (e-mail: fvvi@kth.se; oscarqt@kth.se).

Manuel Arrebola is with the Department of Electrical Engineering, University of Oviedo, ES-33203 Gijón, Spain (e-mail: arrebola@uniovi.es).

Nelson J. G. Fonseca is with the Antenna and Sub-Millimetre Waves Section, European Space Agency, NL-2200 AG Noordwijk, The Netherlands (e-mail: nelson.fonseca@esa.int).

Digital Object Identifier 10.1109/LAWP.2022.3222172

These applications require highly efficient designs and beamforming solutions with propagation in the air are preferred. Fully metallic parallel-plate waveguide (PPW) solutions present low losses and moderate cost [13]. Furthermore, the Luneburg lens [14] is of special interest due to its attractive electromagnetic properties, such as low reflections and rotational symmetry, which means it can be used to cover a wide angular sector with low scan losses [15].

A fully metallic PPW Luneburg lens can be realized using geodesic surfaces [16]. The geodesic surface mimics the response of the Luneburg lens by deforming a PPW section [17], the implementation of such a structure with modulated profiles has been based on subtractive manufacturing methods [18], [19], [20] such as cutting, drilling, or milling. However, manufacturing with these traditional methods does not allow the production of monolithic structures and PPW lenses are typically manufactured in two parts assembled with screws. This can cause some complications (e.g., misalignment between the assembled parts or even leakage), which affect the electromagnetic (EM) performance of the device. In particular, this misalignment was found to increase the level of the sidelobes in the case of the half-Luneburg lens multiple-beam antenna reported in [21].

Additive manufacturing (AM) is a part construction method that has aroused growing interest, generating a booming sector in recent years mainly due to the speed, precision, and versatility it allows compared to traditional manufacturing techniques such as milling. AM consists of depositing layers of material in a controlled manner and can be carried out using different materials such as plastics or, less frequently, metals. AM advantages are being evaluated in multiple fields of application. One of these fields is RF components. For these components, AM came up as a solution to the constraints previously commented because it can be adapted to complex arbitrary shapes. It also relaxes interfaces and flanges design, leading to more compact designs with less or even no screws. Most of the developments that have been proposed to date are based on the use of polymers as a support material on which a metallic coating is subsequently applied to provide the component with conductivity [22] or on the use the polymer itself as a dielectric material [23]. Although this process is qualified for space applications, metal-only parts generally provide better mechanical properties and are preferred for on-board microwave systems. The manufacture of monolithic metal-only waveguide parts could be the solution for the

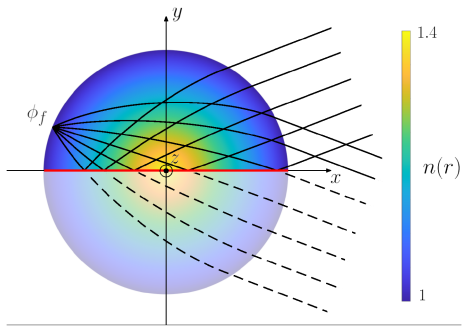

Fig. 1. Illustration of ray-tracing in a half-Luneburg lens (solid lines) compared to ray-tracing in the equivalent full Luneburg lens (dashed lines).

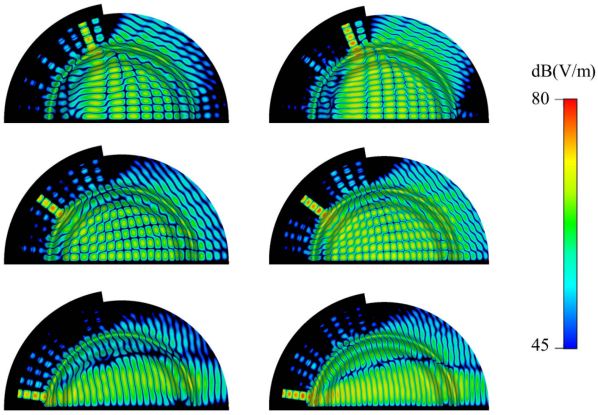

Fig. 2. Simulated electric field distribution (CST Studio Suite) when feeding from different ports at 25 GHz (left) and 29 GHz (right).

misalignment problems when using multiple layers, as observed and suggested for improvement in [21], thus enabling enhanced RF performance at mmWave and above.

Here, a compact and lightweight half-Luneburg lens produced using AM for the first time in a monolithic piece is proposed and experimentally validated. The lens design is the same as in [21] for a fair comparison. A two-step approach is implemented with a first prototype equivalent to the one manufactured using standard milling and a second one taking full advantage of the AM technique to further reduce mass.

II. Half-Luneburg Lens

The refractive index profile $n(r)$ of a planar rotationally symmetric Luneburg lens is defined in the cylindrical coordinate system (r, ϕ, z) with its origin at the center of the lens and its z-axis orthogonal to the plane of the lens as follows [14]:

$$n(r) = \begin{cases} \sqrt{2 - r^2}, & r \leq 1 \\ 1, & r > 1 \end{cases} \quad (1)$$

where r is the normalized radius of the lens. In a half-Luneburg lens design, rays are mirrored using any axis passing through the center of the lens as the symmetry axis, thus, reducing the size of the beamformer while maintaining its focusing properties albeit over a reduced angular range as the resulting design is no longer rotationally symmetric. This is illustrated in Fig. 1 considering the x-axis as symmetry axis. Assuming that the feed angular position ϕ_f may vary from 90° to 180°, angular positions being

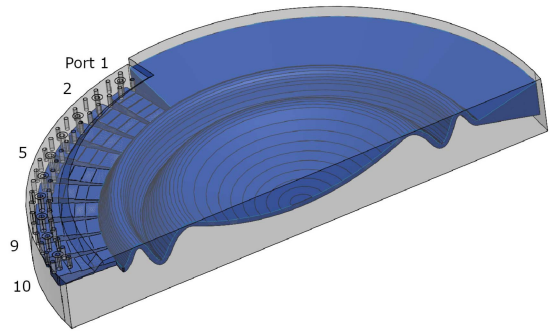

Fig. 3. Full-wave model (blue) of the modulated half-Luneburg geodesic lens, overlaid with the additive manufacturing single-block design (light grey).

defined with reference to the positive x-axis, the corresponding plane wave will be formed in the angular direction ϕ_w ranging from 90° to 0°, respectively. In Fig. 1, the feed position is located at 160°, resulting in a planar wave propagating in the angular direction at 20° with respect to the symmetry axis.

A half-Luneburg lens antenna was analyzed using the frequency domain solver of CST Studio Suite. Electric field distributions provided by the full-wave model are reported in Fig. 2 at 25 and 29 GHz for three different feeding ports (ports 2, 6, and 10 with notations in Fig. 3), showing the wideband operation of the lens, as well as the interference patterns within the PPW section, resulting from the axis symmetry.

III. Additive Manufactured Half-Luneburg Lens Multiple-Beam Antennas

A. Modulated Half-Luneburg Lens in Single-Block

A PPW half-Luneburg geodesic lens, with the modulated profile defined in [19], was presented and validated experimentally in [21]. The mechanical design of the prototype consisted of two plates, top and bottom, which were assembled using 24 screws. Our goal here is joining both plates in a single-block design. By manufacturing a monolithic part, misalignment errors between the two plates can be avoided, hence maintaining good RF performance of the antenna. However, the modulated profile of the lens combined with the multiple feeding ports makes it particularly challenging and the choice of a suitable printing direction is not straightforward. In Fig. 3, the full-wave model of the lens, with vacuum illustrated in blue overlaid with the single-block mechanical design in gray is presented. Since it is a monolithic design, the need for screws to assemble the parts is eliminated, achieving some reduction in volume, mass, and assembly time. The only remaining assembly step needed is for the coaxial connectors. The aperture of the lens, as well as the geodesic shape were kept the same as in [21]. For the inclusion of the coaxial connectors, it was decided to make an initial hole using AM, and then carry out a machining process under which the different transitions are finalized and flanges threaded to ensure good contact for measurement purposes.

In order to compare subtractive and additive manufacturing methods, the single-block prototype previously described was manufactured. This first AM design has similar mechanical characteristics for a fair comparison, except that it is made of a single piece allowing for the removal of the extra material required to insert the screws as well as the screws themselves, reducing the mass by about 23%. As previously mentioned, the

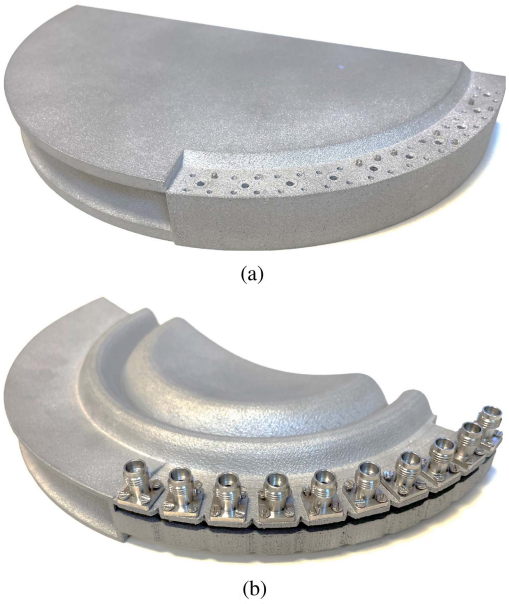

Fig. 4. Prototypes manufactured additively in AlSi10Mg: (a) single-block design (shown without connectors) and (b) compact and lightweight design.

manufacturing of the modulated profile with the feeding ports is not straightforward, therefore, even if the design could be made more compact, thicker walls were kept to ensure manufacturing stability and avoid thermal deformation. This provides a first feasibility demonstration of a monolithic geodesic lens design. The manufacturing process of the single-block prototype was carried out using laser powder-bed fusion (LPBF). The LPBF additive manufacturing technique consists the deposition of powdered material layer by layer in the built plate. It uses a fiber laser as a heat source to selectively scan and melt the material, reaching the desired antenna structure in a monolithic piece. In addition, it shall be considered that high temperatures are reached during the manufacturing process. The manufactured prototype is shown in Fig. 4(a) without connectors to highlight the postmachining of the part required for their inclusion.

B. Compact and Lightweight Modulated Half-Luneburg Lens

After the single-block design, a topological optimization of the antenna was carried out. In this way, the mechanical model was reworked to produce a compact and lightweight design for additive manufacturing. The main drawback of the single-block model in Fig. 4(a), as well as the one presented in [21], lies in their excess material, resulting in an unnecessarily bulky design. This material was not removed in the machined prototype as this requires extra work, thus higher cost. Excess material is also needed to implement the screws for assembling purposes when using conventional subtractive methods. This is not needed when the antenna is manufactured using AM. Furthermore, reduced excess material results in less processing time and bulk material, thus cost savings using AM. Hence, the surrounding block is made here conformal to the geodesic shape, with 2 mm thick walls. A similar thickness is applied to the flare and the feeding part, with the reflective wall and connector area serving to join everything in a single mechanical piece as seen in Fig. 5. Note that the side of the flare horn along the x-axis is closed with metal as also done in [21], thus extending slightly the ground

Fig. 5. Cross-section view of the AM compact and lightweight design (symmetry ground plane removed to show the inner cavity).

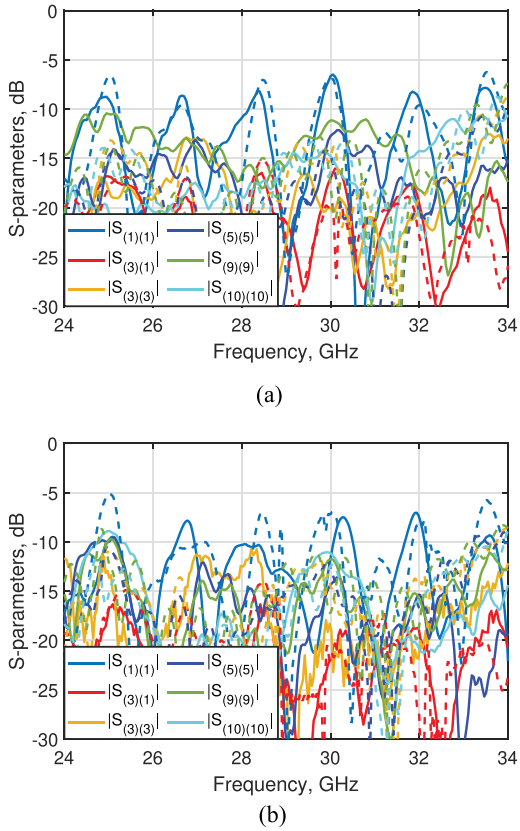

Fig. 6. Selected *S*-parameters (measurements in solid lines and simulations in dashed lines) of the modulated half-Luneburg lens: (a) single-block design and (b) compact and lightweight design.

plane of the half-Luneburg geodesic lens. In order to achieve a correct surface finish that translates into enhanced RF properties, special care was taken in the most delicate parts of the flanges and feed waveguides. In addition, given that the orientation of the manufacturing process is a parameter to be taken into account for the mechanical design, an adaptation was made to the supports of the inlet ports at 45°, a suitable inclination to be printed by additive manufacturing that maintains the rigidity and resistance of the feed zone. Finally, coaxial connectors are used as in previous prototypes, which must be integrated and fastened by means of screws. To do this, the holes of the transitions were made with a certain tolerance in order to subsequently carry out a threading process of these areas by means of machining.

Once the compact and lightweight mechanical model adapted for AM was finalized, its frequency response was simulated once

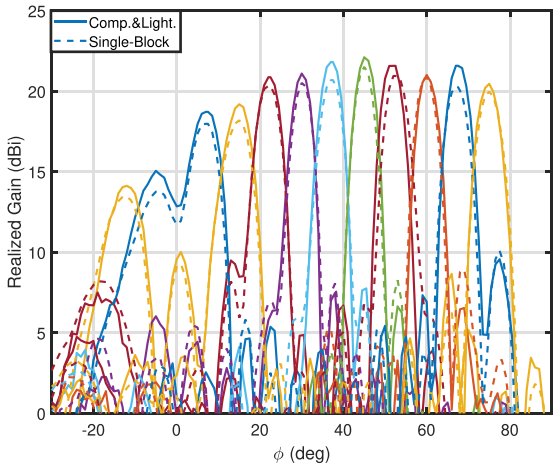

Fig. 7. Measured realized gain patterns of the modulated half-Luneburg geodesic lens at 28 GHz in the beamforming plane (compact and lightweight prototype in solid lines and single-block prototype in dashed lines).

again using CST Microwave Studio to corroborate its correct operation compared to the initial design. The simulation results were as expected, maintaining a complete correlation with the previously simulated prototypes, and the design was manufactured. One important step in the AM process is the cooling stage. The structure may suffer thermal deformations, which may cause unexpected electromagnetic behaviors. To mitigate these possible effects, special care was taken in the design of the parts most prone to thermal deformation, i.e., by increasing or reducing the thickness of these areas. Both prototypes followed the same postprocessing after AM, which consisted in the elimination of manufacturing supports, sandblasting of the complete structure, and threading of flanges. After performing postprocessing stages, a surface roughness of 10 μm is achieved in both prototypes.

IV. Experimental Results

The half-Luneburg geodesic lens antennas were measured in a far-field setup in the anechoic chamber of the Division of Electromagnetic Engineering, KTH. All unused ports were connected with 50-Ω loads. Some selected S-parameters are illustrated for both AM prototypes in Fig. 6. In contrast to results presented in [21], all S-parameters, with the exception of port 1, are below −10 dB over the whole frequency band, showing an improvement over previously reported results. Moreover, port-to-port coupling between ports 1 and 3 remains lower than −16 dB for the whole band for both AM prototypes.

A comparison between measured realized gain patterns at 28 GHz for all ports is provided in Fig. 7. The maximum realized gain, corresponding to the beams pointing at 45°, is 22.1 dBi for the compact and lightweight prototype and 21.5 dBi for the single-block prototype, compared to 21.9 dBi for the milling prototype, as reported in Table I. This confirms that the AM prototypes provide similar gain levels at most ports despite the slightly higher surface roughness when compared to the milling prototype, with gain variations well within tolerances and measurement uncertainties.

As reference, scan losses of the milling prototype were approximately 1.5 dB, considering ports 2–8 thus reducing the scanning range to ±22.5° around the central beam at 45°. Port 1 is not considered here because of the higher return loss and ports 9 and 10 because of the high symmetric lobe. The corresponding scan losses are 1.5 dB and 1.6 dB, respectively, the single-block prototype and the compact and lightweight prototype, indicating very similar operation of all the lenses compared in Table I. The main problem encountered in the previous prototype was a small misalignment of the two halves of the lens, which caused a significant increase in the sidelobe levels for some of the beams. As illustrated in Fig. 8, the AM prototypes significantly overcome this problem. In fact, the sidelobes are reduced by up to 8 dB for the single-block prototype and up to 10 dB for the compact and lightweight prototype considering port 2, with results better aligned with the predictions. These results emphasize the clear benefits of the proposed monolithic implementation.

TABLE I
Comparison of Modulated Half-Luneburg Lenses

Ref.	Design	Weight	Max. Gain[a]	Scan loss[b]
[21]	Milling	1130 g	21.9 dBi	1.5 dB
This Work	Single-Block	871 g	21.5 dBi	1.5 dB
This Work	Comp.&Light.	223 g	22.1 dBi	1.6 dB

[a] Evaluated for port 5, with the beam pointing at 45°.
[b] Evaluated considering ports 2 to 8.

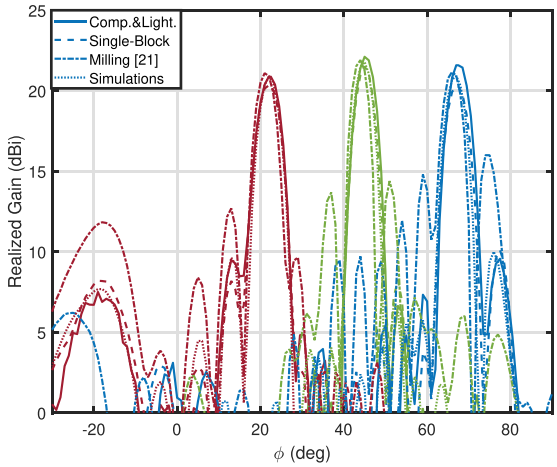

Fig. 8. Selected realized gain patterns of the modulated half-Luneburg geodesic lens at 28 GHz in the beamforming plane (compact and lightweight prototype in solid lines, single-block prototype in dashed lines, milling prototype in dash-dotted lines and simulations in dotted lines).

V. Conclusion

Two prototypes of a PPW half-Luneburg geodesic lens manufactured through additive techniques have been described and validated experimentally showing advantages with respect to the previous design manufactured with milling techniques. Particularly, the compact and lightweight solution presented in this letter maintains the RF performance while displaying a significant reduction in terms of mass. Thus, it is showed that AM techniques, in particular LPBF, are suitable for the manufacturing of metal-only Luneburg lens antennas in a single and lightweight piece. This alternative manufacturing technique solves encountered problems in milling associated with misalignment in assembly.

While these prototypes all implemented the same lens design for a fair comparison, it is anticipated that better RF performance could be reached adapting the modulated lens design and feeding waveguides to the specific constraints of AM. This will be investigated in future works.

REFERENCES

[1] Y. J. Guo, M. Ansari, R. Ziolkowski, and N. J. G. Fonseca, "Quasi-optical multi-beam antenna technologies for B5G and 6G mmwave and THz networks: A review," *IEEE Open J. Antennas Propag.*, vol. 2, pp. 807–830, 2021.

[2] C. Pfeiffer and A. Grbic, "A printed, broadband Luneburg lens antenna," *IEEE Trans. Antennas Propag.*, vol. 58, no. 9, pp. 3055–3059, Sep. 2010.

[3] A. B. Numan, J.-F. Frigon, and J.-J. Laurin, "Printed W-band multibeam antenna with Luneburg lens-based beamforming network," *IEEE Trans. Antennas Propag.*, vol. 66, no. 10, pp. 5614–5619, Oct. 2018.

[4] W. Lee, J. Kim, and Y. J. Yoon, "Compact two-layer Rotman lens-fed microstrip antenna array at 24 GHz," *IEEE Trans. Antennas Propag.*, vol. 59, no. 2, pp. 460–466, Feb. 2011.

[5] Y. J. Cheng et al., "Substrate integrated waveguide (SIW) Rotman lens and its Ka-band multibeam array antenna applications," *IEEE Trans. Antennas Propag.*, vol. 56, no. 8, pp. 2504–2513, Aug. 2008.

[6] N. Jastram and D. S. Filipovic, "Design of a wideband millimeter wave micromachined Rotman lens," *IEEE Trans. Antennas Propag.*, vol. 63, no. 6, pp. 2790–2796, Jun. 2015.

[7] K. Tekkouk, M. Ettorre, L. Le Coq, and R. Sauleau, "Multibeam SIW slotted waveguide antenna system fed by a compact dual-layer rotman lens," *IEEE Trans. Antennas Propag.*, vol. 64, no. 2, pp. 504–514, Feb. 2016.

[8] E. Holzman, "Pillbox antenna design for millimeter-wave base-station applications," *IEEE Antennas Propag. Mag.*, vol. 45, no. 1, pp. 27–37, Feb. 2003.

[9] M. Ettorre, R. Sauleau, and L. Le Coq, "Multi-beam multi-layer leaky-wave SIW pillbox antenna for millimeter-wave applications," *IEEE Trans. Antennas Propag.*, vol. 59, no. 4, pp. 1093–1100, Apr. 2011.

[10] E. Gandini, M. Ettorre, M. Casaletti, K. Tekkouk, L. Le Coq, and R. Sauleau, "SIW slotted waveguide array with pillbox transition for mechanical beam scanning," *IEEE Antennas Wireless Propag. Lett.*, vol. 11, pp. 1572–1575, 2012.

[11] O. Quevedo-Teruel et al., "Geodesic lens antennas for 5G and beyond," *IEEE Commun. Mag.*, vol. 60, no. 1, pp. 40–45, Jan. 2022.

[12] N. J. G. Fonseca, "The water drop lens: Revisiting the past to shape the future," *EurAAP Rev. Electromagn.*, vol. 1, pp. 1–4, Jan. 2022.

[13] T. Ströber, S. Tubau, E. Girard, H. Legay, G. Goussetis, and M. Ettorre, "Shaped parallel-plate lens for mechanical wide-angle beam steering," *IEEE Trans. Antennas Propag.*, vol. 69, no. 12, pp. 8158–8169, Dec. 2021.

[14] R. K. Luneburg and M. Herzberger, "Mathematical theory of optics," *Providence*, 1944, Art. no. 391.

[15] O. Quevedo-Teruel, M. Ebrahimpouri, and F. Ghasemifard, "Lens antennas for 5G communications systems," *IEEE Commun. Mag.*, vol. 56, no. 7, pp. 36–41, Jul. 2018.

[16] R. F. Rinehart, "A solution of the problem of rapid scanning for radar antennae," *J. Appl. Phys.*, vol. 19, no. 9, pp. 860–862, 1948.

[17] K. S. Kunz, "Propagation of microwaves between a parallel pair of doubly curved conducting surfaces," *J. Appl. Phys.*, vol. 25, pp. 642–653, May 1954.

[18] Q. Liao, N. J. G. Fonseca, and O. Quevedo-Teruel, "Compact multibeam fully metallic geodesic Luneburg lens antenna based on non-Euclidean transformation optics," *IEEE Trans. Antennas Propag.*, vol. 66, no. 12, pp. 7383–7388, Dec. 2018.

[19] N. J. G. Fonseca, Q. Liao, and O. Quevedo-Teruel, "Equivalent planar lens ray-tracing model to design modulated geodesic lenses using non-Euclidean transformation optics," *IEEE Trans. Antennas Propag.*, vol. 68, no. 5, pp. 3410–3422, May 2020.

[20] O. Orgeira, G. León, N. J. G. Fonseca, P. Mongelos, and O. Quevedo-Teruel, "Near-field focusing multibeam geodesic lens antenna for stable aggregate gain in far-field," *IEEE Trans. Antennas Propag.*, vol. 70, no. 5, pp. 3320-3328, May 2022.

[21] N. J. G. Fonseca, Q. Liao, and O. Quevedo-Teruel, "Compact parallel-plate waveguide half-Luneburg geodesic lens in the Ka-band," *Microw., Antennas Propag.*, vol. 15, no. 2, pp. 123–130, 2021.

[22] A. Rebollo, A. F. Vaquero, M. Arrebola, and M. R. Pino, "3D-printed dual-reflector antenna with self-supported dielectric subreflector," *IEEE Access*, vol. 8, pp. 209091–209100, 2020.

[23] H. Wang, Q. Chen, O. Zetterstrom, and O. Quevedo-Teruel, "Three-dimensional broadband and isotropic double-mesh twin-wire media for meta-lenses," *Appl. Sci.*, vol. 11, no. 15, 2021, Art. no. 7153.